Mathematical model of tooth flank of worm wheel in globoid worm gear

Matematyczny model boku zęba ślimacznicy przekładni ślimakowej globoidalnej

PIOTR POŁOWNIAK
MARIUSZ SOBOLAK *

DOI: https://doi.org/10.17814/mechanik.2017.1.26

Presented is a mathematical description of tooth flank surface of the wormwheel in globoid worm gear. The kinematic system of tooth formation was performed. The mathematical description of tooth flank of globoid worm was used.

KEYWORDS: globoid worm gear, globoid worm, wormwheel.

The modeling method of worm and wormwheel of globoid worm gear with a rectilinear tooth profile in CAD systems was described by authors in [4-6]. Mathematical model of the globoid worm is described in [3]. The next step is to present a mathematical model of tooth flank of wormwheel in globoid worm gear.

Kinematic system of wormwheel machining using a globoid worm hob

Globoid worm gear is a spiral bevel gear with an axle crossing angle of 90° (Fig. 1) [2]. Fixed motion coordinate systems of a tool x_1 y_1 z_1 and wormwheel shell x_2 y_2 z_2 were introduced. They also included movable systems: $x_1 y_1 z_1$ for tool and $x_2 y_2 z_2$ for wormwheel. The machining worm - tool - rotates around the axis z'_1 by an angle φ_1 opposite to the trigonometric direction. The wormwheel shell rotates around x'_2 axis by an angle φ_2 also in opposition to the trigonometric direction. Centers of coordinate systems are described sequentially with points O_1 and O_2 distant by value a. The surface of the machining worm Σ_1 in the coordinate system x'_1 y'_1 z'_1 is described by the location vector, while the wormwheel surface Σ_2 in the coordinate system x'_1 y'_1 z'_1 – by $\bar{r}_2^{(1')}$. To describe the kinematic system and the tooth profile of machining worm and wormwheel, it is necessary to show the transformations between the systems using a 4 × 4 homogeneous matrices that contain a rotation matrix and a displacement vector (Equations 1-6):

$$M_{11'} = \begin{bmatrix} \cos(\varphi_1) & -\sin(\varphi_1) & 0 & 0 \\ \sin(\varphi_1) & \cos(\varphi_1) & 0 & 0 \\ 0 & 0 & 1 & 0 \\ 0 & 0 & 0 & 1 \end{bmatrix} \quad (1)$$

$$M_{21} = \begin{bmatrix} 1 & 0 & 0 & 0 \\ 0 & 1 & 0 & a \\ 0 & 0 & 1 & 0 \\ 0 & 0 & 0 & 1 \end{bmatrix} \quad (2)$$

$$M_{22'} = \begin{bmatrix} 1 & 0 & 0 & 0 \\ 0 & \cos(\varphi_2) & -\sin(\varphi_2) & 0 \\ 0 & \sin(\varphi_2) & \cos(\varphi_2) & 0 \\ 0 & 0 & 0 & 1 \end{bmatrix} \quad (3)$$

$$M_{12} = \begin{bmatrix} 1 & 0 & 0 & 0 \\ 0 & 1 & 0 & -a \\ 0 & 0 & 1 & 0 \\ 0 & 0 & 0 & 1 \end{bmatrix} \quad (4)$$

$$M_{1'1} = \begin{bmatrix} \cos(-\varphi_1) & -\sin(-\varphi_1) & 0 & 0 \\ \sin(-\varphi_1) & \cos(-\varphi_1) & 0 & 0 \\ 0 & 0 & 1 & 0 \\ 0 & 0 & 0 & 1 \end{bmatrix} \quad (5)$$

$$M_{2'2} = \begin{bmatrix} 1 & 0 & 0 & 0 \\ 0 & \cos(-\varphi_2) & -\sin(-\varphi_2) & 0 \\ 0 & \sin(-\varphi_2) & \cos(-\varphi_2) & 0 \\ 0 & 0 & 0 & 1 \end{bmatrix} \quad (6)$$

where:
$M_{11'}$ – homogeneous transformation matrix from system 1' to 1, M_{21} – homogeneous transformation matrix from the system of fixed machining worm 1 to fixed system of wormwheel 2, $M_{22'}$ – homogeneous transformation matrix from system 2' to 2, M_{12} – homogeneous transformation matrix from the system of fixed wormwheel 2 to fixed system of machining worm 1, $M_{1'1}$ – homogeneous transformation matrix from system 1 to 1', $M_{2'2}$ – homogeneous transformation matrix from system 2 to 2'.

* Mgr inż. Piotr Połowniak (ppolowniak@prz.edu.pl), dr hab. inż. Mariusz Sobolak prof. PRz (msobolak@prz.edu.pl) - Katedra Konstrukcji Maszyn, Wydział Budowy Maszyn i Lotnictwa Politechniki Rzeszowskiej

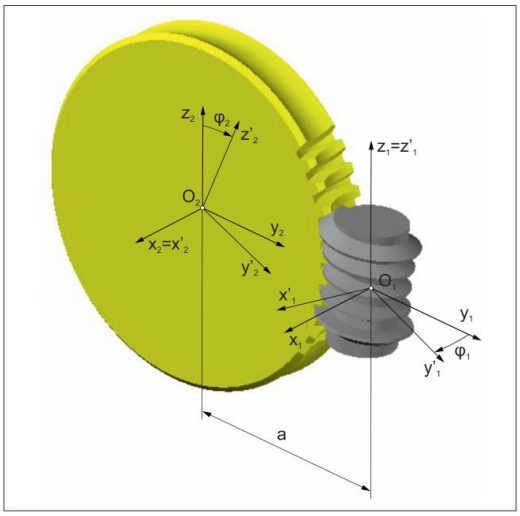

Fig. 1. The kinematic modeling of the tooth flank of a wormwheel in globoid worm gear; $x_1y_1z_1$ – fixed system of a tool (machining worm), $x_2y_2z_2$ – fixed system of a wormwheel shell, $x'_1y'_1z'_1$ – movable system of a tool, $x'_2y'_2z'_2$ – movable system of a wormwheel shell, φ_1 – tool rotation, φ_2 – wormwheel shell rotation, a – distance between tool and wormwheel shell axes

Mathematical model of the tool flank surface – machining worm

Mathematical models of tooth flank in working and machining globoid worm are similar. The difference is that in the tool model, the thickness of the tool tooth and the width of the wormwheel notch must be the same (no circumferential clearance). The parametric description of the tool profile in axial section (Fig. 2) and the globoid helical equation should be used to define the machining worm model. The coordinates of the end points *A* and *B* or *C* and *D* of the profile are determined on the basis of geometric parameters for gear units. The way of their determination was discussed in [3].

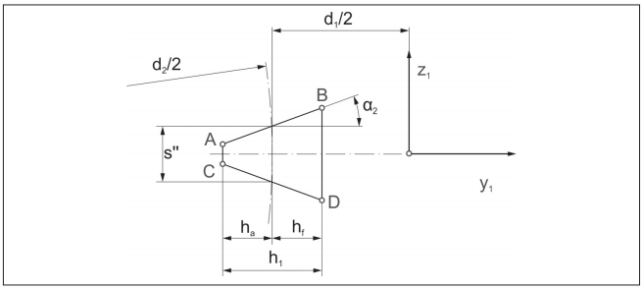

Fig. 2. Fragment of the axial profile of the machining worm for defining the parametric equation of section *AB* or *CD*; *ha* – tooth addendum, h_f – tooth dedendum, h_1 – tool tooth height, *s"* – tooth thickness, α_2 – tool tooth profile angle, d_2 – pitch diameter of wormwheel, d_1 – pitch diameter of machining worm

Parametric equation of the axial profile of the tool in the plane $y_1\,z_1$ is illustrated by the expression [3]:

$$\vec{r}_{AB}^{(1)} = \begin{bmatrix} x_1(u) \\ y_1(u) \\ z_1(u) \\ 1 \end{bmatrix} = \begin{bmatrix} 0 \\ y_{1A} + (y_{1B} - y_{1A}) \cdot u \\ z_{1A} + (z_{1B} - z_{1A}) \cdot u \\ 1 \end{bmatrix} \tag{7}$$

where: y_{1A}, z_{1A} – coordinates of point *A* – start of the profile, y_{1B}, z_{1B} – coordinates of point *B* – end of the profile, u – parameter ($u = u_p$:du:u_k).

Transition of any point in the plane $y_1\,z_1$ along the globoid helix is determined by a homogeneous transformation matrix:

$$M^*_{1'1} = M_{1'1} \cdot M_{12} \cdot M_{2'2} \cdot M_{21} \tag{8}$$

Parametric equation of a tooth flank in globoid machining worm is obtained by moving a tool profile along the globoid helical line. The radial vector of the side surface of the tool is determined by the expression:

$$\vec{r}_1^{(1')} = M^*_{1'1} \cdot \vec{r}_{AB}^{(1)} \tag{9}$$

Once developed, we get [2]:

$$\vec{r}_1^{(1')} = \tag{10}$$

$$= \begin{bmatrix} x_1(u) \cdot \cos(\varphi_1) - a \cdot \sin(\varphi_1) + a \cdot \cos(\varphi_2) \cdot \sin(\varphi_1) + \\ + y_1(u) \cdot \cos(\varphi_2) \cdot \sin(\varphi_1) - z_1(u) \cdot \sin(\varphi_2) \cdot \sin(\varphi_1) \\ -x_1(u) \cdot \sin(\varphi_1) - a \cdot \cos(\varphi_1) + a \cdot \cos(\varphi_1) \cdot \cos(\varphi_2) + \\ + y_1(u) \cdot \cos(\varphi_2) \cdot \cos(\varphi_1) - z_1(u) \cdot \sin(\varphi_2) \cdot \cos(\varphi_1) \\ a \cdot \sin(\varphi_2) + y_1(u) \cdot \sin(\varphi_2) + z_1(u) \cdot \cos(\varphi_2) \\ 1 \end{bmatrix}$$

where: φ_1 – parameter (and worm rotation angle), φ_2 – auxiliary parameter (and wormwheel rotation angle).

Parameter φ_1 specifies the extent of the tool thread. The parameter φ_1 changes from the initial value φ_{1p} to the final value φ_{1k} with step dφ_1. Parameter u changes from the initial value u_p to the final value u_k with the step du. Values dφ_1 and du determine the accuracy of the thread surface in the machining globoid worm. In the equation (10), the dependence $\varphi_2 = \varphi_1 \cdot i$, determined on the basis of the worm gear ratio, should be used:

$$i = \frac{z_1}{z_2} = \frac{\varphi_2}{\varphi_1} \tag{11}$$

where: z_1 – number of worm teeth, z_2 – number of wormwheel teeth.

Mathematical model of wormwheel tooth flank

The surface of the wormwheel tooth flank is the result, among others, of linear contact of the machining worm and processed wormwheel. The fundamental mesh condition is fulfilled:

$$n_x v_x + n_y v_y + n_z v_z = 0 \tag{12}$$

where: n_x, n_y, n_z – components of the vector normal to the surface, v_x, v_y, v_z – components of the vector tangent to the surface.

The inter-tooth contact between the machining worm and the wormwheel can be determined based on the kinematic system shown in Fig. 1. The dependence of the wormwheel shell rotation φ_2 on the machining worm rotation φ_1 is shown by a homogeneous matrix of transformation:

$$M_{2'1'} = M_{2'2} \cdot M_{21} \cdot M_{11'} \tag{13}$$

Substituting equations (1), (2) and (6) to equation (13) gives:

$$M_{2'1'} = \tag{14}$$

$$= \begin{bmatrix} \cos(\varphi_1) & -\sin(\varphi_1) & 0 & 0 \\ -\cos(\varphi_2)\sin(\varphi_1) & \cos(\varphi_2) \cdot \cos(\varphi_1) & -\sin(\varphi_1) & a \cdot \cos(\varphi_2) \\ \sin(\varphi_1)\sin(\varphi_2) & \cos(\varphi_1)\sin(\varphi_2) & \cos(\varphi_2) & a \cdot \sin(\varphi_2) \\ 0 & 0 & 0 & 1 \end{bmatrix}$$

The normal vector in equation (12) can be calculated from the equation of tooth side surface of the globoid machining worm. The normal vector is defined by the expression:

$$\bar{n}_1^{(1')} = L_{2'1'} \cdot \left(\frac{\partial \bar{r}_1^{(1')}}{\partial \varphi_1} x \frac{\partial \bar{r}_1^{(1')}}{\partial u}\right) \tag{15}$$

where: L – transformation matrix from system 1' to 2' – can be obtained by removing the last row and last column of the homogeneous matrix of the equation (14):

$$L_{2'1'} = \begin{bmatrix} \cos(\varphi_1) & -\sin(\varphi_1) & 0 \\ -\cos(\varphi_2)\cdot\sin(\varphi_1) & \cos(\varphi_2)\cdot\cos(\varphi_1) & -\sin(\varphi_1) \\ \sin(\varphi_1)\sin(\varphi_2) & \cos(\varphi_1)\sin(\varphi_2) & \cos(\varphi_2) \end{bmatrix} \tag{16}$$

In the equation (15), the partial derivative $\frac{\partial \bar{r}_1^{(1')}}{\partial \varphi_1}$ is calculated from the equation (10), giving $\varphi_2 = \varphi_1 \cdot i$. The expression $\frac{\partial \bar{r}_1^{(1')}}{\partial u}$ is to be calculated by inserting the parametric equation (7) of the tooth profile $y_1(u)$ and $z_1(u)$ in the equation (10). Expressions $\frac{\partial \bar{r}_1^{(1')}}{\partial \varphi_1}$, $\frac{\partial \bar{r}_1^{(1')}}{\partial u}$ are very complex, therefore they are not expanded here, just like the normal vector $\bar{n}_1^{(1')}$. The tangent vector was calculated based on the system kinematics. The tangent vector is represented by the expression:

$$\bar{v}_1^{(1')} = \frac{\mathrm{d}\bar{r}_{1'}^{(2')}}{\mathrm{d}\varphi_2} = \frac{\mathrm{d}M_{2'1'}}{\mathrm{d}\varphi_2} \cdot \bar{r}_{1'}^{(1')} \tag{17}$$

In equation (17), the derivative $\frac{dM_{2'1'}}{d\varphi_2}$ is calculated from the equation (14) by inserting $\varphi_1 = \frac{\varphi_2}{i}$. Expression expansion is not presented here due to its complexity. In general equation (12), the expressions (15) and (17) are introduced. After solving the equation (12), the set of solutions φ_1 for a given values of the parameter u, is obtained. These parameters determine where there is a linear contact between the worm and wormwheel. After introducing these solutions to equation (10), the contact lines shown in the system x'_1 y'_1 z'_1 of the machining worm, are obtained:

$$\bar{r}_{styk}^{(1')} = \bar{r}_1^{(1')}(\varphi_1, u) \tag{18}$$

The contact lines are shown in Fig. 3 in the system of the machining worm. In much of the gear work cycle, the globoid worm gear geometry creates two contact lines. One contact line is located in the axial plane of the worm (middle section of the wormwheel), is constant and is a straight-line contact. The second contact line is curvilinear, moving toward the first contact line to the overlapping point [1].

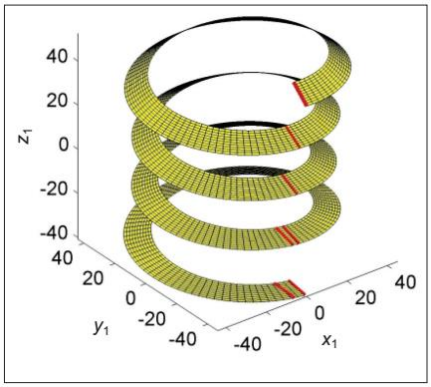

Fig. 3. Contact lines shown on the machining worm flank surface

On the side surface of the wormwheel tooth, three regions are distinguished. Region II is the result of envelope of the tool, while regions I and III are formed by the extreme edge of the tool (Fig. 4) [1, 6].

Region II is obtained by turning the tool by a set value (rotation range from 0 to 2π), defining the tool and wormwheel contact lines as in Fig. 3. The solutions are chosen, which are not in the axial plane of the tool. Then the selected set of solutions should be transfomed to one flank of the wormwheel. An example solution for Region II is shown in Fig. 5. Regions I and III result from shaping the flank surface of the wormwheel by extreme cutting edge of the tool ($r_{1(\varphi_1=\varphi_{1p})}^{(1')}$). It was assumed that the extreme cutting edge in the tool model lies in the plane y_1 z_1 (Fig. 1 and 3). Otherwise, the tool should be rotated by such an angle φ_1 to meet this condition.

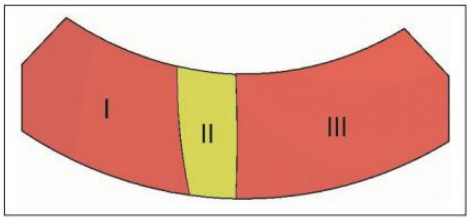

Fig. 4. View of tooth flank in wormwheel with distinguished regions I, II, III [6]

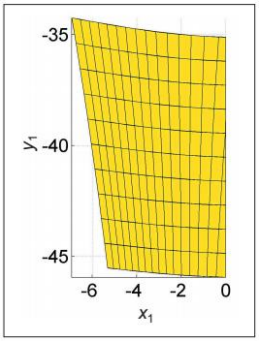

Fig. 5. Region II of the wormwheel tooth flank in the tool system

The surface generated during machining by the extreme edge of the tool in the machining worm system is represented by the expression:

$$\bar{r}_2^{(1')} = M^*_{1'1} \cdot r_{1(\varphi_1=\varphi_{1p})}^{(1')}) \tag{19}$$

In the equation (19) in matrix $M^*_{1'1}$, the range of parameter φ_1 should be chosen so as to obtain the surface of the wormwheel tooth flank with a given width (Fig. 6). This is accomplished by the value φ_{1p}, φ_{1k} with the step $d\varphi_1$.

From the surface in Fig. 6 determined on the basis of equation (19), regions I and III should be separated. The boundaries of the regions are two contact lines in the area of the extreme cutting edge of the tool (Fig. 3). For region I, it is a contact line not included in the axial plane of the tool, for region III, it is the contact line lying in the axial plane of the tool.

The surface of the wormwheel tooth flank is formed by combination of regions I, II and III (Fig. 7).

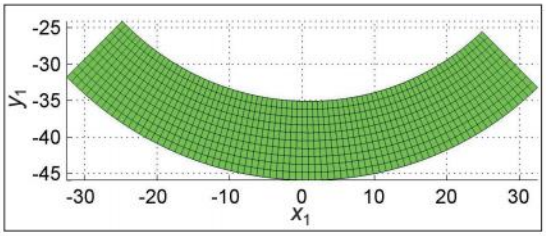

Fig. 6. Surface generated during machining by the extreme edge of the tool

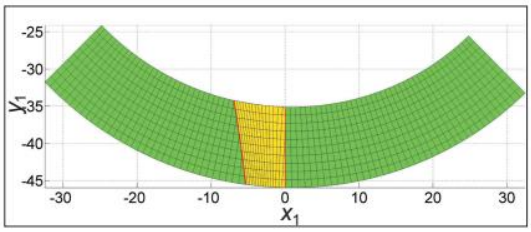

Fig. 7. Surface of the wormwheel tooth flank in globoid worm gear

Conclusions

Defining the mathematical model of a wormwheel in a globoid worm gear is a complex process. After generating the worm and wormwheel lateral surface, the next stage of consideration is the analysis of gear, e.g. the contact pattern.

REFERENCES
1. Litvin Faydor L., Fuentes A. „Double Enveloping Worm Gear Drives". Gear Geometry and Applied Theory. 2-nd ed. Cambridge University Press, 2004.
2. Sabiniak G.H. „Przekładnie ślimakowe". Warszawa: WNT, 2016.
3. Połowniak P., Sobolak M. „Matematyczny model ślimaka globoidalnego na potrzeby generowania modelu CAD". Mechanik. 2 (2015): CD.
4. Połowniak P., Sobolak M. „Modelowanie ślimaka globoidalnego w środowisku CAD". Mechanik. 1 (2015): pgaes 71–74.
5. Połowniak P., Sobolak M. „Modelowanie ślimacznicy przekładni ślimakowej globoidalnej w środowisku CAD". Mechanik. 3 (2015): pages 250–252.
6. Połowniak P., Sobolak M. „Wpływ skrajnej krawędzi frezu ślimakowego na kształtowanie boku zęba ślimacznicy". Mechanik. 7 (2015): pages 625–627.